J. Phys. Chem. A **1998,** *102,* 9489−9493 **9489**

A New Application of the Interaction Picture To Calculate Reactive Scattering Matrix Elements

Michael J. MacLachlan[†] **and David E. Weeks***

Department of Engineering Physics, Air Force Institute of Technology, 2950 P Street,
Wright-Patterson AFB, Ohio 45433

Received: April 24, 1998; In Final Form: July 13, 1998

The interaction picture is used together with the channel-packet method in a new time-dependent approach to compute reactive scattering matrix elements. The channel-packet method employs the correlation function between two Møller states to compute scattering matrix elements. The interaction picture reduces wavepacket spreading when computing the Møller states. The details of this new approach are illustrated using a simple one-dimensional example where the size of the grid required for computing the Møller state in the interaction picture is reduced by a factor of 2 when compared with required grid size in the Schrödinger picture.

1. Introduction

Reactive scattering-matrix(S-matrix) elements yield the probability that reactants in a given initial asymptotic reactant state will collide and scatter into products in a final asymptotic product state.[1−3] For reactants with two or more degrees of freedom, the calculation of S-matrix elements is numerically intensive, and various time-dependent wavepacket techniques have been developed in an effort to reduce the required computational effort.[4−12] A primary weakness shared by these time-dependent methods is the large grid required to support the evolving wavepacket before it enters the interaction region of the potential, as well as after it exits the interaction region and spreads out into one or more arrangement channels. One approach for reducing the required grid size employs the interaction picture to propagate the wavepackets with less spreading than occurs in the Schrödinger picture.

Previous use of the interaction picture has been limited to half-reactions involving a single arrangement channel.[3,13−16] The principal difficulty in extending the interaction picture to treat multichannel reactive scattering has been the absence of a single asymptotic Hamiltonian suitable for all arrangement channels involved in the reaction.[3] In this paper, we describe a new technique for computing S-matrix elements that surmounts this difficulty by using the interaction picture together with the recently developed channel-packet method.[17−19]

The channel-packet method enables the use of the interaction picture for computing reactive S-matrix elements by splitting the computational effort into two parts. In the first part, asymptotic reactant and product wavepackets are individually propagated into the interaction region of the potential. Since the asymptotic reactant wavepacket is propagated independently of the product wavepacket, it is possible to choose an asymptotic Hamiltonian and corresponding interaction picture that is well suited for the reactant arrangement channel. In a similar fashion, the asymptotic product wavepacket is propagated independently of the reactant wavepacket, and it is possible to choose an asymptotic Hamiltonian and corresponding interaction picture well suited for the product arrangement channel. By using two different interaction pictures, one for the reactant arrangement channel and one for the product arrangement channel, it is possible to realize savings in the required grid size similar to those previously achieved in the non-reactive half-collisions.[16] During the second part of the channel-packet method, the reactant and product wavepackets obtained from the first part of the calculation are further propagated using the Schrödinger picture. The time-dependent correlation between the evolving wavepackets is calculated as they bifurcate into energetically accessible arrangement channels and are absorbed using absorbing boundary conditions.[20−26] A simple one-dimensional example is used to illustrate the essential features of this new approach.

2. The Channel Packet Method

The time-dependent channel-packet method is used to compute S-matrix elements in the momentum representation. This is accomplished by constructing an initial reactant channel packet, $|\psi_{\text{in}}^{\gamma}\rangle$, in the coordinate representation, from the direct product of an internal reactant eigenstate, labeled γ, with a linear combination of plane waves describing the relative motion of the reactants and products. The channel packet $|\psi_{\text{in}}^{\gamma}\rangle$ is propagated backward in time using an asymptotic Hamiltonian, $\mathbf{H}_a^{\gamma}$, that correctly describes the dynamics of the reactants in the γ-channel asymptotic limit where they are widely separated and noninteracting. The resulting state is then propagated forward in time using the full scattering Hamiltonian, $\mathbf{H}$, yielding the reactant Møller state, $|\psi_{+}^{\gamma}\rangle$. In a similar fashion, an initial product channel packet, $|\psi_{\text{out}}^{\gamma'}\rangle$, is constructed in the coordinate representation. The product channel packet is propagated forward in time using an asymptotic Hamiltonian that properly describes the asymptotic dynamics of the products, and then backwards in time using the full Hamiltonian. This sequence of propagations is motivated by the Møller-operator formulation of scattering theory,[3] where

$$|\psi_{\pm}^{\gamma}\rangle = \mathbf{\Omega}_{\pm}^{\gamma}|\psi_{\substack{\text{in}\\\text{out}}}^{\gamma}\rangle = \lim_{t\to\mp\infty}\,[\mathrm{e}^{i\mathbf{H}t/\hbar}\mathrm{e}^{-i\mathbf{H}_a^{\gamma}t/\hbar}]|\psi_{\substack{\text{in}\\\text{out}}}^{\gamma}\rangle \qquad (2.1)$$

[†] Now at Air Force Research Laboratory, AFRL/PRS, 10 E. Saturn Blvd., Edwards AFB, CA 93524.

10.1021/jp981991u

$\Omega_{\pm}^{\gamma}$ are Møller operators, and the scattering operator,

$$\mathbf{S}^{\gamma'\gamma} = \mathbf{\Omega}_{-}^{\gamma'\dagger}\mathbf{\Omega}_{+}^{\gamma} \tag{2.2}$$

As discussed in greater detail in the next section, the asymptotic Hamiltonian $\mathbf{H}_{a}^{\gamma}$, used to propagate the reactant channel packet $|\psi_{\text{in}}^{\gamma}\rangle$, provides the transformation from the Schrödinger picture to an interaction picture well suited for computing the reactant Møller state $|\psi_{+}^{\gamma}\rangle$. Similarly, the asymptotic Hamiltonian $\mathbf{H}_{a}^{\gamma'}$, used to propagate the product channel packet $|\psi_{\text{out}}^{\gamma'}\rangle$, provides the transformation from the Schrödinger picture to an interaction picture well suited for computing the product Møller state $|\psi_{-}^{\gamma}\rangle$. The time-dependent correlation between $|\psi_{+}^{\gamma}\rangle$ and $|\psi_{-}^{\gamma}\rangle$

$$C^{\gamma'\gamma}(t) = \langle\psi_{-}^{\gamma'}|\mathrm{e}^{-i\mathbf{H}t/\hbar}|\psi_{+}^{\gamma}\rangle \tag{2.3}$$

is computed in the Schrödinger picture and then used to calculate S-matrix elements,

$$\mathrm{S}_{\pm k'\gamma',\pm k\gamma}^{\gamma',\gamma} = \frac{\hbar}{2\pi\eta_{-}^{*}(\pm k_{\gamma'}')\,\eta_{+}(\pm k_{\gamma})}\left[\frac{|k_{\gamma'}'||k_{\gamma}|}{\mu_{\gamma'}\mu_{\gamma}}\right]^{1/2}\int_{-\infty}^{\infty}\mathrm{d}t \times \exp\left\{\frac{iEt}{\hbar}\right\}C^{\gamma'\gamma}(t) \tag{2.4}$$

where the $\eta(k)$ are expansion coefficients of the plane waves used to construct the initial wavepackets and the μ are reduced masses corresponding to the reactant and product arrangement channels.

There have been several applications of the channel-packet method to a variety of scattering problems. In particular, the method has been used to compute state to state S-matrix elements for the collinear $\mathrm{H} + \mathrm{H_2}(n) \leftrightarrow \mathrm{H_2}(n') + \mathrm{H}$ reaction[19,26] and more recently for a two-dimensional model $\mathrm{OC} + \mathrm{OH}$-$(n{=}0) \leftrightarrow \mathrm{OCO}(n{=}0) + \mathrm{H}$ reaction.[28] In a larger three-dimensional calculation, Dai and Zhang have used the channel-packet method to compute exact state-to-state S-matrix elements for the $\mathrm{H} + \mathrm{O_2}$ reaction.[10] One common advantage shared by all of these calculations is the facility with which the channel-packet method provides S-matrix elements over a wide range of energies. In addition to exact quantum calculations, the channel-packet method has also been useful in formulating several approximate strategies for computing S-matrix elements. These include a new semiclassical method for computing S-matrix elements developed by Garashchuk and Tannor,[29] and the application of the multiconfiguration time-dependent Hartree approach to computing S-matrix elements by Jäckle and Meyer.[30]

3. Application of the Interaction Picture

The transformation from the Schrödinger picture to the interaction picture is

$$|\psi^{\gamma}(t)\rangle_{\mathrm{I}} = \mathrm{e}^{i\mathbf{H}_0^{\gamma}t/\hbar}|\psi^{\gamma}(t)\rangle_{\mathrm{S}} \tag{3.1}$$

where the subscript I labels the interaction picture and the subscript S refers to the Schrödinger picture.[31] It is seen readily from eq 3.1 that $|\psi(0)\rangle_{\mathrm{I}} = |\psi(0)\rangle_{\mathrm{S}}$. The operator $\mathbf{H}_0^{\gamma}$ may be any portion of the full Hamiltonian, where

$$\mathbf{H} = \mathbf{H}_0^{\gamma} + \mathbf{H}_1^{\gamma} \tag{3.2}$$

Typically, $\mathbf{H}_0^{\gamma} = \mathbf{p}^{\gamma^2}/2\mu$, where $\mathbf{p}^{\gamma}$ is the momentum conjugate to the Jacobi coordinate describing the relative separation between reactants or products. The interaction-picture Hamiltonian is then defined as

$$\mathbf{H}_{\mathrm{I}}^{\gamma}(t) = \mathrm{e}^{i\mathbf{H}_0^{\gamma}t/\hbar}\mathbf{H}_1^{\gamma}\mathrm{e}^{-i\mathbf{H}_0^{\gamma}t/\hbar} \tag{3.3}$$

and the time-evolution operator is

$$\mathbf{U}_{\mathrm{I}}^{\gamma}(t, t_0) = \mathrm{e}^{i\mathbf{H}_0^{\gamma}t/\hbar}\mathrm{e}^{-i\mathbf{H}(t,t_0)/\hbar}\mathrm{e}^{-i\mathbf{H}_0^{\gamma}t_0/\hbar} \tag{3.4}$$

Since Møller states are defined in the Schrödinger picture at time $t = 0$, they are equal to their counterparts in the interaction picture:

$$|\psi_{\pm}^{\gamma}\rangle_{\mathrm{I}} = |\psi_{\pm}^{\gamma}\rangle_{\mathrm{S}} \tag{3.5}$$

The initial asymptotic reactant and product states are also equivalent

$$|\psi_{\substack{\text{in}\\ \text{out}}}^{\gamma}\rangle_{\mathrm{I}} = |\psi_{\substack{\text{in}\\ \text{out}}}^{\gamma}\rangle_{\mathrm{S}} \tag{3.6}$$

Therefore, if the interaction picture is constructed with $\mathbf{H}_0^{\gamma} = \mathbf{p}^{\gamma^2}/2\mu$, a free-particle Hamiltonian, the Møller states are obtained by a simple propagation in the interaction picture

$$|\psi_{\pm}^{\gamma}\rangle_{\mathrm{I}} = \lim_{t\to\mp\infty}\mathbf{U}_{\mathrm{I}}^{\gamma\dagger}(t)|\psi_{\substack{\text{in}\\ \text{out}}}^{\gamma}\rangle_{\mathrm{I}} \tag{3.7}$$

The channel-packet method thus enables the use of different interaction pictures most appropriate for each channel, since reactant and product Møller states are propagated independently.

In order to realize a reduction in grid size when computing Møller states,we employed the PR-adapted “nested” interaction picture.[32] The PR-adapted nested interaction picture shifts the origins of both the momentum (P) and the coordinate (R) representations, defining the state vector,

$$|\psi\rangle_{\mathrm{I}}'' = \mathrm{e}^{i\langle\mathbf{R}\rangle\mathbf{P}_{\mathrm{S}}/\hbar}\mathrm{e}^{-i\langle\mathbf{P}\rangle\mathbf{R}_{\mathrm{S}}/\hbar}\mathrm{e}^{i\mathbf{H}_0t/\hbar}|\psi\rangle_{\mathrm{S}} \tag{3.8}$$

where $\langle\mathbf{R}\rangle = \langle\psi|_{\mathrm{I}}\mathbf{R}_{\mathrm{I}}|\psi\rangle_{\mathrm{I}} = \langle\psi|_{\mathrm{S}}\mathbf{R}_{\mathrm{S}}|\psi\rangle_{\mathrm{S}}$ is the expectation value of the position operator, and $\langle\mathbf{P}\rangle$ is the expectation value of the momentum operator. Wavepackets can be propagated using fewer grid points in the PR-adapted interaction picture because they remain centered on the grid in both the momentum and coordinate representations.

The PR-adapted equation of motion is given by

$$i\hbar\frac{\mathrm{d}}{\mathrm{d}t}|\psi\rangle_{\mathrm{I}}'' = \mathbf{H}''|\psi\rangle_{\mathrm{I}}'' \tag{3.9}$$

where

$$\mathbf{H}'' = \mathrm{e}^{i\langle\mathbf{R}\rangle\mathbf{P}_{\mathrm{S}}/\hbar}\mathrm{e}^{-i\langle\mathbf{P}\rangle\mathbf{R}_{\mathrm{S}}/\hbar}\mathrm{e}^{i\mathbf{H}_0^{\gamma}t/\hbar}\mathbf{H}_1^{\gamma}\mathrm{e}^{-i\mathbf{H}_0^{\gamma}t/\hbar}\mathrm{e}^{i\langle\mathbf{P}\rangle\mathbf{R}_{\mathrm{S}}/\hbar}\mathrm{e}^{-i\langle\mathbf{R}\rangle\mathbf{P}_{\mathrm{S}}/\hbar} \tag{3.10}$$

An iterated Lanczos propagator[8] is used in the interaction picture because of the time dependence of (3.10). To improve the accuracy of the propagator for a given time step Δt, the time-

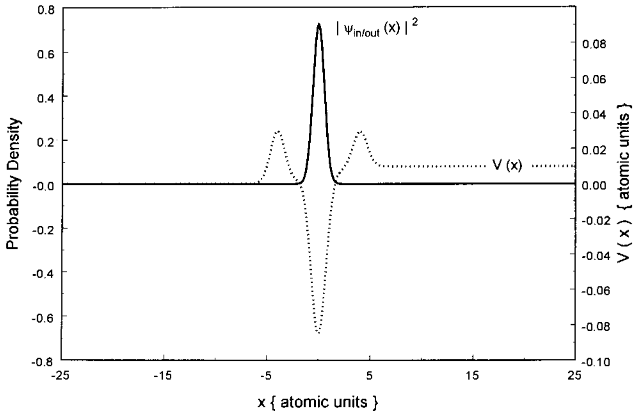

Figure 1. Initial channel packets $\psi_{\mathrm{in}}(x)$ and $\psi_{\mathrm{out}}(x)$ (solid line) are the same in the interaction and Schrödinger pictures, since they are evaluated at $t = 0$. The potential (dotted line) is given by eq 4.1, where the asymptotic Hamiltonian to the right of the interaction region of the potential differs from the asymptotic Hamiltonian to the left by a constant potential offset $V_0 = 0.01$ atomic units.

evolution operator can be approximated with a second-order truncation of the Magnus expansion[16,33]

$$U_{\mathrm{I}}''(t_{k+1},t_k) = \exp\left\{-\frac{i}{\hbar}\int_{t_k}^{t_{k+1}}\mathbf{H}_{\mathrm{I}}''(t')\,\mathrm{d}t' - \frac{1}{2\hbar^2}\int_{t_k}^{t_{k+1}}\mathrm{d}t'\int_{t_k}^{t'}[\mathbf{H}_{\mathrm{I}}''(t'),\mathbf{H}_{\mathrm{I}}''(t'')]\,\mathrm{d}t'' + \ldots\right\} \approx \exp\left\{-\frac{i}{\hbar}\mathbf{H}_{\mathrm{I}}''\left(t_k + \frac{\Delta t}{2}\right)\Delta t - \frac{1}{12\hbar^2}[\mathbf{H}_{\mathrm{I}}''(t_{k+1}),\mathbf{H}_{\mathrm{I}}''(t_k)](\Delta t)^2\right\} \quad (3.11)$$

An iterative application of U_{I}'' on $|\psi^{\gamma}_{\substack{\mathrm{in}\\ \mathrm{out}}}\rangle$ yields the Møller states $|\psi^{\gamma}_{\pm}\rangle$.

4. S-Matrix Elements via the Channel-Packet Method in the Interaction Picture

We illustrate the interaction-picture channel-packet technique using a one-dimensional potential,

$$V(x) = A\mathrm{e}^{-\alpha(x-a)^2} - B\mathrm{e}^{-\beta(x-b)^2} + C\mathrm{e}^{-\gamma(x-c)^2} + D\Theta(x-a)\Theta(c-x)x + V_0\Theta(x-a) \quad (4.1)$$

where $\Theta(x)$ represents a Heaviside step function. This potential, shown using the dotted lines in Figures 1–3, is chosen to schematically represent the reaction path of a reactive molecular collision that has two different asymptotic Hamiltonians. For $x \to -\infty$, the asymptotic Hamiltonian is

$$\mathbf{H}_a^{\mathrm{L}} = \mathbf{p}^2/2\mu \quad (4.2)$$

and for $x \to +\infty$, the asymptotic Hamiltonian is

$$\mathbf{H}_a^{\mathrm{R}} = \mathbf{p}^2/2\mu + V_0 \quad (4.3)$$

The values used for the parameters in eq 4.1 are given in Table 1.

The initial coordinate representation of the product and reactant wavepackets shown in Figure 1 is a Gaussian,

$$\langle x|\psi^{\gamma}_{\mathrm{in(out)}}\rangle = [2\pi\sigma^2]^{-1/4}\exp\left[-\frac{(x-x_0)^2}{4\sigma^2} + ik_0x\right] \quad (4.4)$$

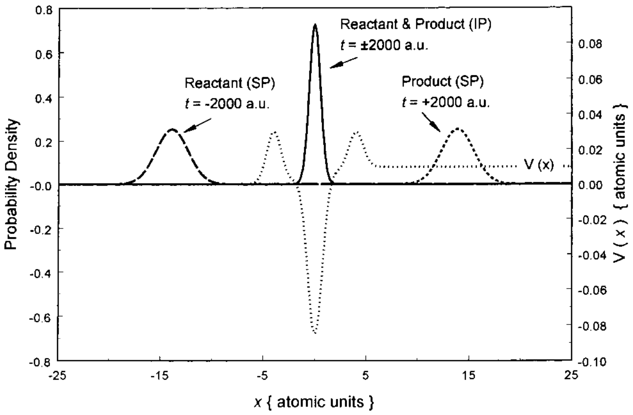

Figure 2. Reactant channel packet propagated backward in time to $t = -2000$ atomic units, and the product channel packet propagated forward in time to $t = 2000$ atomic units. Since the propagation occurs under a free-particle Hamiltonian, the wavepackets are unaffected in the interaction picture (solid line). In the Schrödinger picture (dashed lines) the reactant and product wavepackets translate and spread, requiring a larger grid.

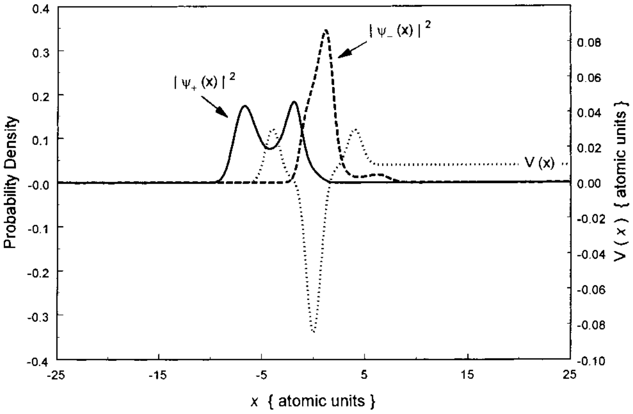

Figure 3. Reactant Møller state, $\psi_+(x)$ (solid line), and the product Møller state, $\psi_-(x)$ (dashed line), are obtained by propagating the intermediate reactant and product states forward and backward, respectively, to time $t = 0$.

TABLE 1: Coefficients Used in Eq 4.1 To Create the Potential Function That Appears in Figures 1–3[a]

potential coefficients					
A	0.03	a	−4.0	α	1.0
B	0.09	b	0.0	β	1.0
C	0.02	c	4.0	γ	1.0
D	0.00125				

[a] All quantities are in atomic units.

TABLE 2: Coefficients Used in Eq 4.2 To Create the Asymptotic Wavepackets Shown in Figure 1[a]

wavepacket coeff	
x_0	0.0
k_0	8.5
σ	0.55
μ	1224

[a] All quantities are in atomic units.

The choice of $+k_0$ in eq 4.4 will yield the probability, as a function of kinetic energy, that reactants approaching from the left will form products exiting to the right. The values of the coefficients used in eq 4.4 are given in Table 2. In the Schrödinger picture, the first propagation in eq 2.1 is performed analytically,[34] using the initial wavepackets together with $\mathbf{H}_a^{\mathrm{L}}$

TABLE 3: Quantities Associated with the Generation of the Intermediate States in Figure 2 and the Møller States in Figure 3[a]

	Moller-state propagation
t	±2000
t_0	0
Δt	0.5
Δx	0.1
N	256

[a] All quantities are in atomic units.

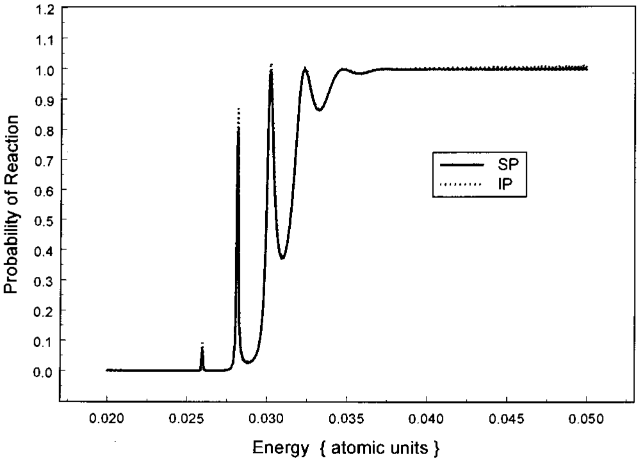

Figure 4. Probability of reaction computed in the interaction picture (dotted line) and the Schrödinger picture (solid line). The interaction-picture S-matrix elements were computed on a grid half the size required for the Schrödinger-picture matrix elements.

and $\mathbf{H}_a^R$ to obtain intermediate reactant and product wavepackets, respectively. As shown in Figure 2, these wavepackets have both translated and spread relative to the initial wavepackets. Typically, this wavepacket translation and spreading in the Schrödinger picture generates a requirement for large grids. However, in the interaction picture, the intermediate wavepackets do not translate or spread, and remain identical to the initial wavepackets. Figure 2 also illustrates the intermediate interaction-picture channel packets and demonstrates that they require a smaller grid when compared with the intermediate Schrödinger-picture wavepackets. In the interaction picture, the intermediate wavepackets are used in eq 3.7 together with the appropriate asymptotic Hamiltonian to compute the reactant and product Møller states. The Møller states shown in Figure 3 were computed on a grid of 256 points using the nested interaction picture with a second-order Lanczos propagator and a four-dimensional Krylov subspace. Constants used for the propagation are listed in Table 3. For comparison,the same Møller states were computed in the Schrödinger picture, requiring a grid of 512 points.

To complete the calculation, the Møller states were propagated in the Schrödinger picture using a split-operator propagator together with absorbing boundary conditions to compute the correlation function in eq 2.3.[26,27] S-matrix elements were then computed using eq 2.4, resulting in the probability for reaction shown in Figure 4. For comparison, the probability of reaction computed entirely within the Schrödinger picture is also shown in Figure 4.

It is important to note that since short iterative Lanczos propagation is employed when using the nested interaction picture, a greater number of FFTs is required per time step when compared to the split-operator approach commonly used for time-independent Hamiltonians in the Schrödinger picture. This results in a trade-off between the computational savings afforded by the grid reduction, and the requirement for a larger number of FFTs per time step. An alternative to the short iterative Lanczos propagator that avoids this trade-off is the second-order finite difference propagation technique developed by Zhang.[13,35] Using this approach, the number of FFTs per time step is reduced to the same number required by the split-operator method. This second-order finite difference technique has been successfully applied to a two-dimensional model of CH_3I photodissociation,[36] and to a three-dimensional model of vibrational predissociation of van der Waals molecules.[37]

5. Conclusion

Through the use of the channel-packet method, the interaction picture can be used to compute reactive scattering matrix elements on reduced computational grids. Previous use of the interaction picture has been restricted to single scattering channels, limiting its application to nonreactive scattering problems. The channel-packet method opens the possibility of extending the efficacy of the interaction picture by allowing each Møller state to be computed in an interaction picture derived from its asymptotic Hamiltonian. In the simple one-dimensional illustration given here, a 2-fold reduction in required grid size has been demonstrated.

Acknowledgment. We dedicate this paper to R. D. Levine on the occasion of his 60th birthday, and one of us (D.E.W.) is thankful for the opportunity to have worked as a postdoc with Prof. Levine. This work is supported in part by the Air Force Office of Scientific Research and by the Aeronautical Systems Center Major Shared Resource Center.

References and Notes

(1) Levine, R. D. *Quantum Mechanics of Molecular Rate Processes*; Oxford University Press: Oxford, UK, 1969.
(2) Levine, R. D.; Bernstein, R. B. *Molecular Reaction Dynamics*; Oxford University Press: New York, 1974.
(3) Taylor, J. R. *Scattering Theory: The Quantum Theory of Nonrelativistic Collisions*; Krieger: Malabar, FL, 1987.
(4) Kosloff, R.; Kosloff, D. *J. Chem. Phys.* **1983**, *72*, 1823.
(5) Gerber, R. B.; Kosloff, R.; Berman, M. *Comput. Phys. Rep.* **1986**, *5*, 59.
(6) Kosloff, R. *J. Phys. Chem.* **1988**, *92*, 2087.
(7) Judson, R. S.; Kouri, D. J.; Neuhauser, D.; Baer, M. *Phys. Rev. A* **1990**, *42*, 351.
(8) Leforestier, C.; Bisseling, R. H.; Cerjan, C.; Feit, M. D.; Friesner, R.; Guldberg, A.; Hammerich, A.; Jolicard, G.; Karrlein, W.; Meyer, H.-D.; Lipkin, N.; Roncero, O.; Kosloff, R. *J. Comput. Phys.* **1991**, *94*, 59.
(9) Sharafeddin, O.; Zhang, J. Z. H. *Chem. Phys. Lett.* **1993**, *204*, 190.
(10) Dai, J.; Zhang, J. Z. H. *J. Phys. Chem.* **1996**, *100*, 6898.
(11) Schatz, G. C. *J. Phys. Chem.* **1996**, *100*, 12839.
(12) Zhu, W.; Zhao, X.; Tang, Y. *J. Chem. Phys.* **1996**, *106*, 2271.
(13) Zhang, J. Z. H. *J.Chem.Phys.* **1989**, *92*, 324.
(14) Zhang, J. Z. H. *Chem. Phys. Lett.* **1989**, *160*, 417.
(15) Das, S.; Tannor, D. J. *J. Chem. Phys.* **1990**, *92*, 3403.
(16) Williams, C. J.; Qian, J.; Tannor, D. J. *J. Chem. Phys.* **1991**, *95*, 1721.
(17) Tannor, D. J.; Weeks, D. E. *J. Chem. Phys.* **1993**, *98*, 3884.
(18) Weeks, D. E.; Tannor, D. J. *Chem. Phys. Lett.* **1993**, *207*, 301.
(19) Weeks, D. E.; Tannor, D. *J. Chem. Phys. Lett.* **1994**, *224*, 451.
(20) Kosloff, R.; Cerjan, D. *J. Chem. Phys.* **1984**, *81*, 3722.
(21) Neuhauser, D.; Baer, M. *J. Chem. Phys.* **1989**, *91*, 4651.
(22) Neuhauser, D.; Baer, M. *J. Chem. Phys.* **1989**, *90*, 4351.
(23) Neuhauser, D.; Baer, M.; Judson, R. S.; Kouri, D. *J. Comput. Phys. Commun.* **1991**, *63*, 460.
(24) Balint-Kurti, G. G.; Vibok, A. In *Numerical Grid Methods and Their Application to Schrödinger's Equation*; Cerjan, C., Ed.; Kluwer Academic: Dordrecht, 1993.
(25) Riss, U. V.; Meyer, H.-D. *J. Chem. Phys.* **1996**, *105*, 1409.
(26) Calfas, R.; Weeks, D. E. *Chem. Phys. Lett.* **1996**, *263*, 292.

(27) Calfas, R. *Reactive Quantum Scattering in Two Dimensions*. Ph.D. Dissertation, Air Force Institute of Technology, 1997.

(28) Weeks, D. E.; Calfas, R. S. Proceedings of the High Energy Density Matter Contractors Conference, 20 May 1998, Monterey, Ca, in press.

(29) Garashchuk, S.; Tannor, D. *J. Chem. Phys. Lett.* **1996**, *262*, 477.

(30) Jäckle, A.; Meyer, H.-D. *J. Chem. Phys.* **1995**, *102*, 5650.

(31) Shankar, R. *Principles of Quantum Mechanics*; Plenum: New York, 1980.

(32) Tannor, D. J.; Besprozvannaya, A.; Williams, C. J. *J. Chem. Phys.* **1992**, *96*, 2998.

(33) Magnus, W. *Commun. Pure Appl. Math.* **1954**, *7*, 649.

(34) Merzbacher, E. *Quantum Mechanics*; Wiley: New York, 1970.

(35) Zhang, J. Z. H. *Comput. Phys. Commun.* **1991**, *63*, 28.

(36) Zhang, D. H.; Sharafeddin, O. A.; Zhang, J. Z. H. *Chem. Phys.* **1992**, *167*, 137.

(37) Zhang, D. H.; Zhang, J. Z. H. *J. Phys. Chem.* **1992**, *96*, 1575.